The Journal of Experimental Biology 204, 785–795 (2001)
Printed in Great Britain © The Company of Biologists Limited 2001
JEB3142

DETECTION OF Cl^- FLUX IN THE APICAL MICROENVIRONMENT OF CULTURED FOETAL DISTAL LUNG EPITHELIAL CELLS

S. C. LAND* AND A. COLLETT

Centre for Research into Human Development, Tayside Institute of Child Health, Ninewells Hospital and Medical School, Dundee DD1 9SY, Scotland, UK

*e-mail: s.c.land@dundee.ac.uk

Accepted 30 November 2000; published on WWW 1 February 2001

Summary

A self-referencing Cl^--selective microelectrode (Cl^- SrE) was developed and used to detect changes in the direction and magnitude of the Cl^- flux (J_{Cl}) from the apical region of cultured foetal distal lung epithelial cells (FDLEs) as a function of external Cl^- concentration ($[Cl^-]_e$) and in response to pharmacological challenges. The technique, which is similar to that developed for other ion-selective microelectrodes, centres on the oscillation of a Cl^--selective microelectrode between known points, micrometres apart, orthogonal to the plasma membrane. Application of the Fick principle to the differential voltage obtained per excursion amplitude (the referenced signal) yields the Cl^- flux (pmol cm^{-2} s^{-1}). A Cl^- effusion gradient was used to confirm that empirical measurements of J_{Cl} using the Cl^- SrE were statistically similar to predicted flux values calculated from the fall in $[Cl^-]$ with distance from the tip of the effusion source. Apical J_{Cl} was then measured as a function of $[Cl^-]_e$ from polarised FDLE cultures grown on permeable supports. At $[Cl^-]_e$<50 mmol l^{-1}, an apical-to-basolateral (inward) flux, maximal at 400 pmol cm^{-2} s^{-1}, was observed; this reverted to a continuous basolateral-to-apical (outward) flux of 203 pmol cm^{-2} s^{-1} at $[Cl]_e$>100 mmol l^{-1}. At $[Cl^-]_e$>100 mmol l^{-1}, isoproterenol (basolaterally applied, 10 μmol l^{-1}) activated a Cl^- influx of 561 pmol cm^{-2} s^{-1}, whereas UTP (apically applied, 100 μmol l^{-1}) stimulated a Cl^- efflux of 300 pmol cm^{-2} s^{-1}. In all cases, 50–70 % of J_{Cl} was abolished by Cl^- channel blockade using 10 μmol l^{-1} diphenylamine-2-carboxylic acid (DPC) or 5-nitro-2-(3-phenylpropylamino)benzoic acid (NPPB). We conclude that the Cl^- SrE resolves a Cl^- gradient in the microenvironment of the apical region of lung epithelia that varies in both direction and magnitude as a function of external $[Cl^-]_e$ and in response to Cl^- channel blockade and to β_2 adrenoreceptor and P2Y receptor agonists.

Key words: self-referencing electrode, fluid transport, lung, cystic fibrosis, β_2 adrenoreceptor, P2Y receptor, Cl^- flux.

Introduction

Fluid transport in lung epithelia is governed by the regulated flux of Na^+ and Cl^-, which generate the osmotic force for fluid transfer from one side of the epithelial barrier to the other. Whereas Na^+/K^+-ATPase activity provides the electrogenic energy that drives this process, the transmembrane distribution of Na^+ and Cl^- is determined by ligand-regulated ion channels and exchangers which, if defective, result in diseases associated with dysfunctional fluid transport. The ionic composition of the external medium (i.e. the airway surface liquid, ASL) within the respiratory tree is, therefore, a major determinant of the physiological performance of the lung in health and disease (Boucher, 1999).

As defective Cl^- transport is causative in the pathophysiology of cystic fibrosis, considerable effort has gone into determining the physiological range of Cl^- concentration ($[Cl^-]$) in ASL (Baconnais et al., 1999; Boucher, 1994; Hull et al., 1998; Knowles et al., 1997; Matsui et al., 1998). Gross measurements of ASL, however, reveal little information regarding the actual $[Cl^-]$ within the microenvironment of epithelial cells since this presumably varies as a function of diffusion distance from fluid-secreting glands or, indeed, pathways of Cl^- entry and exit *via* tight junctions and channels within the apical membrane itself. With uncertainty as to the precise level of physiological $[Cl^-]$ within the macro- and micro-environments of the membrane, the assessment of processes governing Cl^- transport and their pharmacological manipulation requires an understanding of the local Cl^- flux over a broad range of external Cl^- concentrations ($[Cl^-]_e$).

Techniques used to characterise the primary signalling pathways that regulate Cl^- entry and exit from lung epithelial cells generally involve either indirect detection of anion transport as a component of total ion transport (e.g. the measurement of short-circuit current) or gross direct measurement by isotope tracer techniques. Although these approaches are powerful, they lack temporal and spatial signal resolution and, consequently, convey little information about

the transport of a given ion as a function of its concentration in the microenvironment of the plasma membrane.

The self-referencing electrode (SrE) technique overcomes these limitations by using a single ion-selective microelectrode (tip diameter approximately 3–5 μm), continuously oscillated orthogonal to the plasma membrane, to record a differential voltage that changes in proportion to the transport of the selected ion species. Application of the Fick principle to the differential voltage obtained (ΔμV) per amplitude (μm) of electrode excursion yields a measure of flux (pmol cm^{-2} s^{-1}). Signal referencing in this manner provides an additional operational advantage by effectively filtering out inherent noise, drift or interference. Since the original voltage 'vibrating' probe was developed by Jaffe and Nuccitelli (Jaffe and Nuccitelli, 1974), the SrE principle has been adapted for use with both cationic-selective microelectrodes (Ca^{2+}, H^+, K^+) (Kuhtreiber and Jaffe, 1990; Smith et al., 1994; Breton et al., 1996; Land et al., 1997; Shirihai et al., 1998; Smith and Trimarchi, 2000) and polarographic (O_2) microelectrodes (Land et al., 1999; Trimarchi et al., 2000) on samples ranging in magnitude from single isolated cells to tissues.

Here, we report the development of a Cl^--selective self-referencing (SrE) microelectrode suited for the real-time, high-resolution, non-invasive detection of Cl^- flux direction and magnitude over broad ranges of external [Cl^-]. As little is known about the role of surface liquid composition in the regulation of fluid transport in the distal lung, we used polarised monolayers of foetal distal lung epithelial cells (FDLEs) to test the capacity of the Cl^- SrE to detect Cl^- transport in response to basolateral (β_2 adrenoreceptor) or apical (purinoreceptor) agonists that evoke changes in the direction and magnitude of Cl^- transport. Our results demonstrate the presence of a Cl^- gradient within the microenvironment of the apical membrane that is intimately linked to the physiology of fluid transport in the distal lung.

Materials and methods

Isolation and culture of foetal distal lung epithelial cells

All procedures requiring the use of rats were pre-approved by the Committee for Animal Care and Experimentation at the host institution for these experiments [Marine Biological Laboratory (MBL), Woods Hole, MA 02543, USA]. Time-mated pregnant female Sprague Dawley rats were purchased from Charles River (MA, USA) and housed in the animal care facility at the MBL. At day 20 of gestation (term is 22 days), the animals were killed by cervical dislocation, and the foetuses were removed by caesarean section and immediately decapitated. Foetal mass (minus lung tissue) was 2.12±0.13 g (mean ± S.E.M., *N*=12 litters), which matches the range expected for rat foetuses at 19 days post-conception out of a 22-day gestation period (Schellhase et al., 1989).

The foetal lungs were removed, dissected free of major airways and extraneous tissues, finely minced, and then washed free of erythrocytes by rinsing several times in ice-cold sterile Ca^{2+}- and Mg^{2+}-free Hanks balanced salt solution (HBSS). The cleaned lung tissue was resuspended in HBSS containing 0.02 % (w:v) trypsin and 0.012 % (w:v) DNAase I at a volume of 1 ml per foetus and incubated with agitation at 37 °C for 20 min. At the end of this period, the solution was centrifuged at 100 ***g*** for 2 min to remove undispersed tissue from cells, and the supernatant was transferred into a fresh sterile tube. An equal volume of Dulbecco's modified Eagle's medium (DMEM) with 10 % foetal calf serum (FCS) was added to the supernatant to neutralise proteolytic activity. To maximise yield, the digestion protocol was repeated on the remaining tissue fragments. After filtering the supernatant through a 120 μm sterile nylon mesh, the filtrate was centrifuged at 420 ***g*** for 5 min. The cell pellet was resuspended in 20 ml of DMEM containing 10 % (v:v) FCS, and the cells were placed into a T-150 culture flask at 37 °C to enable fibroblasts and non-epithelial cells to adhere to the culture flask for 1 h (repeated once). At the end of this period, unattached cells were centrifuged at 130 ***g*** for 3 min, and the pettet was resuspended in 20 ml of DMEM (without FCS) before repeating the centrifugation. Cells were washed four times, after which the supernatant was discarded. At the end of the fourth wash, the cells were counted and seeded onto 1 cm diameter Transwell clear (Corning Costar Alewife, MA, USA) permeable supports (0.4 μm pore size) at a density of 1.5×10^6 cells per membrane. Adherent cells were washed with 20 ml DMEM 24 h later and placed into 2 ml of serum-free PC-1 medium (Biowhittaker). We have found that cells plated this way typically possess transepithelial resistances (R_t) greater than 300 Ω cm^2 and a transepithelial potential difference of 4.3±0.2 mV (mean ± S.E.M., *N*=110; S. M. Wilson, personal communication).

Cl^- self-referencing electrodes

Patch-style microelectrodes with a tip diameter of 3 μm were constructed from borosilicate glass as described previously (Smith et al., 1994). The electrodes were back-filled with 100 mmol l^{-1} NaCl, 10 mmol l^{-1} Tris/H_2SO_4 (pH 7.4) and then front-filled with a 300 μm column length of 5,10,15,20-tetraphenyl-21H,23H-porphin manganese(III)chloride [Mn(III)TPPCl^-; Cl^- ionophore I-Cocktail A (Fluka)] (Kondo et al., 1989). The electrode was connected to a motion-controlled head stage *via* a Ag/AgCl wire, and the circuit was completed by placing a salt bridge (3 mol l^{-1} sodium acetate in agar connected to a Ag/AgCl wire) submerged in the medium at the edge of the dish. The entire assembly was mounted on the stage of a Zeiss inverted microscope housed in a Faraday cage. Details of motion control, signal detection and amplification devices have been reported previously (Kuhtreiber and Jaffe, 1990; Smith et al., 1994; Land et al., 1999) and are products of the BioCurrents Research Center (Marine Biological Laboratory, Woods Hole, MA 02543, USA: www.mbl.edu/BioCurrents). Electrode movements about the cell were monitored throughout each experiment with the aid of a video monitor.

Nernstian calibration of the electrode was conducted by recording the millivolt signal difference in 0.1, 1, 10 and 100 mmol l^{-1} solutions of NaCl buffered with 10 mmol l^{-1}

Tris/H_2SO_4 to pH 7.4. Electrode calibration was typically linear over this range, yielding a slope of –60.4 mV per decade [Cl^-] (r^2=0.98). Electrode resistance was determined by Ohm's law by passing a 5 mV pulse over the sensor column in the tip of the microelectrode and measuring the resulting current. This method was appropriate for the measurement of resistance because we found no change in resistance values, column length or integrity of the sensor material with repeated pulsing over several minutes. Electrode drift was monitored over the course of each experiment by following the change in the direct current signal per hour.

Experimental design

Experiments were divided into three parts.

Part A: characterisation of Cl^- SrE performance

The characteristics with which the electrode measures Cl^- flux were determined by creating a steady-state Cl^- diffusion gradient from an artificial point source. Briefly, a micropipette with a tip diameter of 3 μm was filled with a solution of 0.5 % agar containing 100 mmol l^{-1} NaCl. The bulk solution around the tip of the pipette consisted of 100 mmol l^{-1} Na^+ as the prevalent cation in 0.1 mol l^{-1} sodium-phosphate-buffered saline (five volumes of Na_2HPO_4 to one volume of NaH_2PO_4, pH 7.4). In this way, interference from osmotic and bulk liquid flow around the tip of the point source was minimised and a steady-state Cl^- gradient was established after approximately 1 h. To determine the characteristics of Cl^- flux detection, Cl^--selective electrodes were progressively moved outwards within the gradient to known positions orthogonal to the tip of the point source. At each position, a direct voltage signal was obtained with the electrode motionless, followed by measurement of a differential voltage with the electrode oscillating over 8 μm. Signals obtained at points throughout the Cl^- gradient in both motionless and oscillating formats were compared by conversion to Cl^- concentration difference (μmol cm^{-3}) in the same manner as described previously for Ca^{2+} self-referencing microelectrodes (Kuhtreiber and Jaffe, 1990) using the relationship derived in the legend to Fig. 1. Signal filtering and data collection rate are described below.

Part B: detection of Cl^- flux from rat FDLEs in monolayer culture

The outlines of individual cells comprising the epithelial monolayer were clearly visible through the base of the Transwell clear permeable support (see Fig. 2A); hence, by using the electrode motion control, it was possible to position the tip of the electrode within 1 μm of the apical membrane of any given cell. Once the point of closest approach had been established, the electrode was oscillated at a frequency of 0.3 Hz over an amplitude (r) of 10 or 20 μm in the vertical (z) plane. Cl^--specific signal differences (ΔμV) obtained over the amplitude of the electrode excursion were corrected for background Cl^- concentration and converted to a Cl^- concentration differential (ΔC, μmol cm^{-3}) using the equation:

$$\Delta C = 2.3(\Delta V/[i]_e)/S, \quad (1)$$

where ΔV is the signal difference (mV) measured over the amplitude of electrode oscillation, $[i]_e$ is the background concentration of Cl^- (=$[Cl^-]_e$) in the medium (μmol cm^{-3}), which was continuously measured as a direct current signal throughout each experiment and S is the Nernstian calibration slope of the electrode. Multiplication by 2.3 converts the Nernstian calibration from base 10 to natural logarithms (as derived by Kuhtreiber and Jaffe, 1990). These values were then converted to a directional measurement of flux by substitution into the Fick equation:

$$J_{Cl} = D(\Delta C/\Delta r), \quad (2)$$

where J_{Cl} is the flux of Cl^- (mol cm^{-2} s^{-1}), D is the aqueous diffusion coefficient for Cl^- at 25 °C (5.8×10^{-6} cm^{-2} s^{-1}) and Δr is the amplitude of electrode oscillation (cm). Note that the error arising from electrode drift, which is associated with the continuous measurement of $[i]_e$, was negligible over our experimental period (Table 1).

Part C: pharmacological manipulation of the Cl^- flux signal

Experiments were conducted over a range of Cl^- concentrations by washing filters free from PC-1 medium and replacing it with 0.1 mol l^{-1} sodium-phosphate-buffered saline (5 volumes of Na_2HPO_4 to 1 volume of $NaH_2PO_4{\cdot}H_2O$, pH 7.4) containing (in mmol l^{-1}): 40 NaCl, 5 KH_2PO_4, 0.8 $MgSO_4$, 0.5 $CaCl_2$ and 5 Na^+-glucose. The osmolality of this solution (308 mosmol kg^{-1}) was close to that of PC-1 medium (297 mosmol kg^{-1}). The concentration of Cl^- was set at the desired level by varying the concentration of NaCl in solution and compensating for osmotic imbalance with sodium mannitol, leaving HPO_4^{2-} as the dominant anion. The times of addition and concentration of blockers, agonists and antagonists are as described in the figure legends.

Data handling and statistical analyses

Data were collected using Ionview software (BioCurrents Research Center, Marine Biological Laboratory, Woods Hole,

Table 1. *Electrode performance and calibration*

Parameter	
Drift (mV h^{-1})	
Bulk medium	0.09±1.8 (40)
At cell	0.22±1.3 (40)
Resistance (GΩ)	16.5±0.7 (6)
Nernstian calibration*	
0 mmol l^{-1} $NaHCO_3$	x=–60.4log[Cl^-]–48.6 (r^2=0.98) (40)
5 mmol l^{-1} $NaHCO_3$	x=–60.5log[Cl^-]–41.2 (r^2=0.98) (40)
50 mmol l^{-1} $NaHCO_3$	x=–32.5log[Cl^-]–18.8 (r^2=0.88) (5)

*Nernstian calibration performed in 0.1, 1, 10, 100 mmol l^{-1} NaCl, 10 mmol l^{-1} Tris/H_2SO_4, pH 7.4.

Values are mean ± S.E.M. with the number of repetitions shown in parentheses.

x, signal difference (mV); [Cl^-] is in mol l^{-1}.

MA, USA) as described previously (Kuhtreiber and Jaffe, 1990; Smith et al., 1994; Land et al., 1999). Briefly, signals were collected at a rate of 1000 data points per second from an electrode translated in a square wave at a rate of 0.3 Hz. The signal at each extreme of the translation was separated into 10 bins each averaged from 166 data points. The first three data bins obtained at either extreme were discarded to eliminate movement artefacts, with the remaining data bins being used to obtain the differential signal. Significant differences between groups were assessed by one-way analysis of variance (ANOVA) followed by Dunnett's test, with confidence limits set at 95 %. The value of N is the number of cell preparations from each pregnant female rat used in each experiment.

Chemicals

Chloride ionophore I-cocktail A was purchased from Fluka (Buchs, Switzerland), ultrapure uridine and adenosine 5′-triphosphates were from Pharmacia (Little Chalfont, Bucks, UK), 5-nitro-2-(3-phenylpropylamino)benzoic acid (NPPB) and diphenylamine-2-carboxylic acid (DPC) were from ICN (Basingstoke, Hants, UK). All other chemicals were purchased from Sigma (St Louis, MO, USA, and Poole, Dorset, UK). Culture media consisted of PC-1 (Biowhittaker, Bakersville, MD, USA), and DMEM and HBSS were purchased from Life-Sciences (Rockville, MD, USA).

Results and discussion

Electrode properties

The performance characteristics of Mn(III)TPP-tipped microelectrodes are given in Table 1 and are broadly similar to those reported previously (Kondo et al., 1989). Note that the resistance value obtained falls within the range for other ionophore-tipped microelectrodes (5×10^{10} to $3\times10^{11}\,\Omega$; Smith et al., 1994). Nernstian calibration yielded a slope of –60.4 mV per 10-fold change in Cl^- concentration, which was used to calculate $[Cl^-]_e$ and subsequent values of J_{Cl} over the time course of each experiment. For this to be justified, it was important to establish that drift was a negligible component of the overall signal. The average rate of drift in the non-referenced voltage output during cellular measurements was $0.22\,mV\,h^{-1}$ (Table 1) amounting to 0.3 % of the millivolt difference obtained per decade change in Cl^- concentration. As no single electrode was used for more than 3 h, we consider drift to be a negligible component of $[i]_e$. The selectivity of the electrode sensor material for Cl^- over HCO_3^- represents a second possible area for signal bias. Mn(III)TPP possesses a Nicolsky–Eisenmann selectivity coefficient ($\log K^{pot}_{Cl,HCO_3}$) of –1.62 (Kondo et al., 1989), indicating a selectivity for Cl^- that is 43 times greater than for HCO_3^-. Approximations of HCO_3^- flux calculated from lung and renal epithelial preparations suggest that upper limits will reside between 0.17 and $0.36\,nmol\,cm^{-2}\,s^{-1}$ (Illek et al., 1997; Muller-Berger et al., 1999; Tsuruoka and Schwartz, 1999). If we take into account the 43-fold difference in selectivity, the latter would account for 2.1–3.7 % of the spontaneous Cl^- flux signals we observed at $[Cl^-]_e$ values above $100\,mmol\,l^{-1}$ and is, therefore, considered negligible.

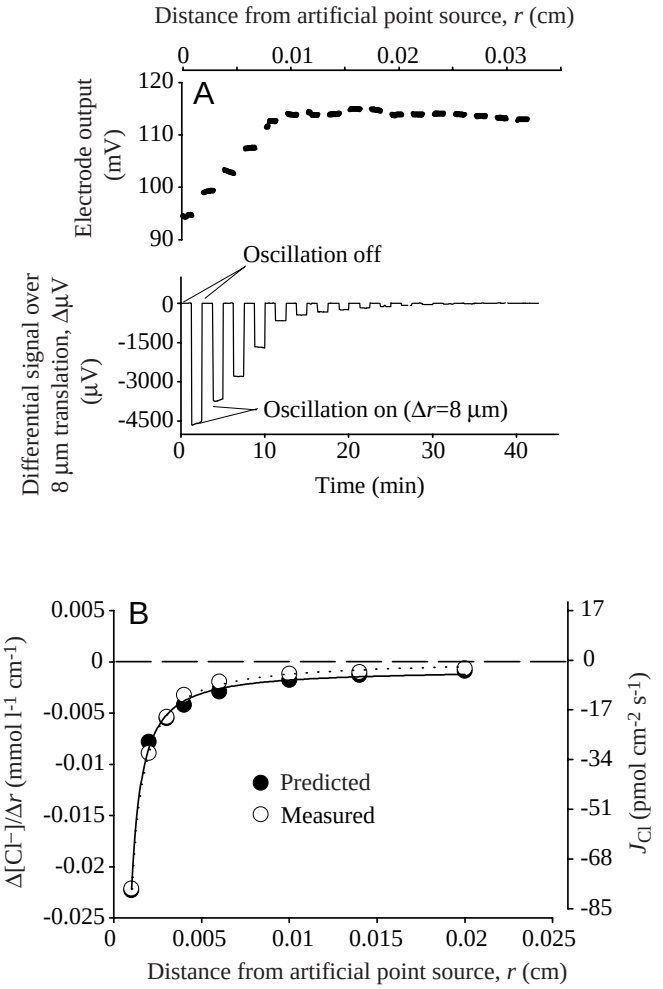

Fig. 1. Comparison of measured and predicted signal differences in an artificially constructed Cl^- gradient radiating from an artificial source with a tip diameter of 3 μm containing $100\,mmol\,l^{-1}$ NaCl in a bathing medium of $100\,mmol\,l^{-1}$ Na_2HPO_4:NaH_2PO_4 (5:1) at 25 °C. (A) Representative experiment showing the change in electrode output with distance from the tip of the point source (upper graph) and the corresponding differential signal (ΔμV) obtained over an oscillation of 8 μm (lower graph). (B) Signal difference (expressed as concentration difference divided by the amplitude of oscillation) calculated from the relationship derived by Kuhtreiber and Jaffe (1990), $\Delta V=S[(-K\Delta r)/([i]_e r^2+Kr)]/2.3$, where ΔV is the voltage difference (mV), S is the Nernstian calibration slope of the Cl^- electrode, K is a constant derived from the least-squares regression of the change in signal with distance through the artificial gradient ($\mu mol\,cm^{-2}$), Δr is the amplitude of electrode oscillation (cm), r is the distance from the point source (cm) and $[i]_e$ is the background concentration of Cl^- ($\mu mol\,cm^{-3}$). There was no statistical difference between the regression slopes of the two lines, as determined by least-squares analysis. The measured data points (open circles) represent the means ± S.E.M. (bars fall within symbols) of 25 data points collected at each position. J_{Cl}, Cl^- flux.

A third possible area affecting detection sensitivity concerns the response time of the electrode. The 10–90 % response times

reported previously (Kondo et al., 1989) for Mn(III)TPP microelectrodes with a tip diameter of 1 μm range between 11 and 41 s depending on the amplification equipment used. No detail is provided as to how stepwise changes in [Cl^-] concentration were achieved in solution to achieve an 80 % change in the maximal signal. In our experiments, we found it was not possible to create stepwise changes in [Cl^-] in solution without introducing errors resulting from excessive flow or from mechanical or thermal disturbances. Introducing the electrode from the air into a solution containing 10 mmol l^{-1} NaCl (buffered with 10 mmol l^{-1} Tris/H_2SO_4, pH 7.5) produced a 0–90 % response time of 10.4 s, which incorporates the same errors. We believe, therefore, that the response time of the sensor material is not reliably reported but is significantly less than 10 s for a microelectrode with a tip diameter of 3–5 μm. Confirmation that our operating criteria (i.e. rate and amplitude of electrode oscillation, rate of data collection and processing) were sufficient for quantifiable detection of Cl^- flux was obtained using an artificial Cl^- effusion gradient as described in the next section.

Cl^- flux measurement from an artificial source

To determine the efficiency with which Cl^--selective microelectrodes detect Cl^- flux when operated in a self-referencing format, we constructed an artificial Cl^- diffusion gradient that could be used to determine both the efficiency and detection sensitivity of the technique. Fig. 1A (upper graph) demonstrates the change in signal intensity measured with a stationary Cl^--selective microelectrode when it is moved to positions outwards from a 100 mmol l^{-1} NaCl point source. The slope of change in Cl^- concentration with distance r (cm) from the orifice of the artificial point source, given by $y=K\log_e x-a$, was used to determine the predicted signal differential between any two points within the gradient (where K is the slope and a is the intercept). By returning the electrode to each position throughout the artificial Cl^- gradient and oscillating it at 0.3 Hz over 8 μm (Fig. 1A, lower graph), the empirically determined signal differential (i.e. the referenced signal) could then be compared with that predicted from the slope obtained from the static measurements. As referencing the voltages obtained from either extreme of the oscillation effectively filters interference resulting from noise and electrode drift, a signal differential should theoretically be detectable within a shallow gradient even when static electrode measurements over the same distance do not register a significant change. This was broadly the case with our experiments, as both panels of Fig. 1A demonstrate: a substantial signal differential was measured at points in the gradient that yielded little detectable change in the static voltage measurements.

Fig. 1B demonstrates a close (no statistical difference; $F_{1,6}$, $P<0.001$, H_o: $\beta_{Theoretical}=\beta_{Measured}$ accepted) match between the predicted signal differential and that measured using the same electrode in a self-referencing format over the range of subsequently measured biological signal differentials (<1ΔmV). Errors associated with the determination of r increased with proximity to the mouth of the artificial source, so data collected from this region were omitted for the calculation of the slope of each relationship. Note that, as Cl^- radiates outwards from the tip of the artificial source, a negative signal differential denotes a net Cl^- efflux and, conversely, a positive signal differential denotes a net Cl^- influx. For the purposes of measurements conducted on FDLE monolayers, an efflux is interpreted as basolateral-to-apical transport and an influx as apical-to-basolateral transport, with flux in both cases interpreted as net ionic movement through both intracellular and paracellular pathways.

Detection of Cl^- flux from rat FDLEs

The Nernstian properties of ion-selective electrodes can place a considerable limit upon the degree to which definitive signals can be obtained in the presence of physiological concentrations of the specific ion of interest in bulk solution. Our aim was directly to measure the flux Cl^- across the plasma membrane at various values of $[Cl^-]_e$, so it was important to ensure (i) that the operating range of the Cl^--selective microelectrode covered the breadth of [Cl^-] reported in airway surface liquid (ASL) and (ii) that the substitute anion species did not significantly interfere with the measurement of J_{Cl} by participating in its transport pathways.

The range of [Cl^-] reported in ASL in normal and diseased conditions such as cystic fibrosis is highly variable and relates largely to fluid obtained from the larger airways (77–108 mmol l^{-1}, Hull et al., 1998; 65–83 mmol l^{-1}, Becconnais et al., 1999); 125 mmol l^{-1}, Knowles et al., 1997). The liquid ion exchanger employed here remains responsive to Cl^- concentrations up to 0.21 mol l^{-1} (abscissa intercept value with 5 mmol l^{-1} external bicarbonate; Table 1), so it should be possible to detect voltage differences from cells maintained in buffers that span the broad reported range of ASL [Cl^-]. We used HPO_4^{2-} as a convenient substitute anion species because it is relatively impermeable to the apical membrane of epithelial cells, possessing a low selectivity ratio with respect to Cl^- and other halides in apical anion-conductance pathways (Illek et al., 1999). Moreover, the reported value of K^{pot}_{Cl,HPO_4} for Mn(III)TPP (–2.93) suggests that this liquid ion exchanger is highly selective for Cl^- over HPO_4^{2-}. Indeed, the presence of 100 mmol l^{-1} HPO_4^{2-} in the bulk solution did not appreciably quench the Cl^- efflux detected from artificial NaCl point sources, nor were we able to measure an appreciable signal differential from an artificial point source containing 100 mmol l^{-1} Na_2HPO_4 in agar with distilled water as the bulk solution (S. C. Land, unpublished observation).

Foetal distal lung epithelial cells maintained in monolayer culture demonstrated spontaneous transmembrane transport of Cl^-, the direction of which was dependent on the external Cl^- concentration ($[Cl^-]_e$). The differential signal diminished with distance as the electrode was moved to positions above and away from the apical plasma membrane (Fig. 2B) but was repeatedly attained by returning the electrode to its original position of approach at the cell (inset). A definitive background (zero signal differential) measurement was not obtained until the electrode was more than 20 μm above the cell, so electrode excursions shorter than this were within the extracellular Cl^- gradient. ΔC_{Cl}

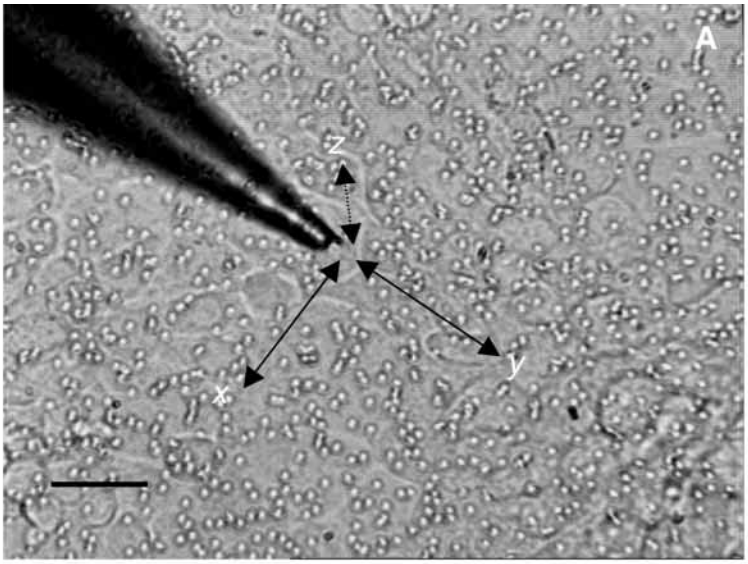

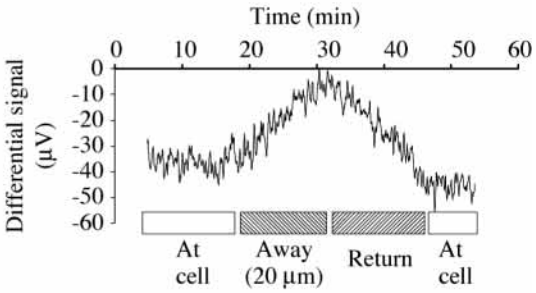

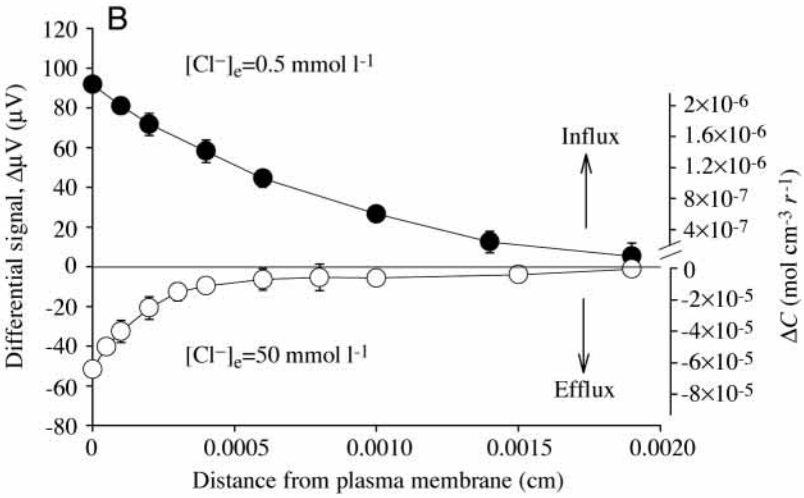

Fig. 2. (A) Visual representation of a foetal distal lung epithelial cell (FDLE) monolayer (basolateral view) cultured on a 0.4 μm pore size Transwell clear (Costar) permeable support. The tip of the Cl^--selective microelectrode is shown 2 μm above (*z* plane) a cell within the FDLE monolayer, and the *x*, *y* (horizontal) and *z* (vertical) planes of oscillation are represented by arrows. Pores in the polystyrene membrane support are clearly visible as bright speckles. Scale bar, 10 μm. (B) Complementary representative experiments (repeated five times) showing the direction and magnitude of the extracellular signal differential (ΔμV) obtained with a single Cl^--selective microelectrode oscillated over 10 μm at 0.3 Hz in the *z* plane at increasing distances above a single FDLE cell. Increasing $[Cl^-]_e$ from 0.5 to 50 mmol l^{-1} produced a change in the direction of the signal from Cl^- influx to efflux. Values are means ± S.E.M. of 25 data points collected at each position. The inset to B portrays a representative experiment in which the electrode was moved slowly (at approximately 2 μm min^{-1}) in the *z* plane through the Cl^- gradient of a Cl^--secreting cell to a point 20 μm above the apical membrane. The electrode was then returned at the same rate towards the original measuring position orthogonal to the apical membrane. Δ*C*, Cl^- concentration differential.

calculated from the signal differential data confirms (i) that a concentration gradient for Cl^- exists relative to the apical membrane, and (ii) that both the direction and magnitude of this gradient change as a function of Cl^- concentration in the bulk medium. These data prove that the molar concentration of Cl^- in the bulk solution is an inadequate descriptor of $[Cl^-]$ in the microenvironment of the apical membrane itself.

Fig. 3 demonstrates the effect of $[Cl^-]_e$ on the direction and magnitude of the spontaneously generated signal differential measured from unstimulated cells over a 10 μm electrode oscillation orthogonal to the apical membrane (*z* plane). Note that the ΔμV differential signal (Fig. 3A) does not take into account the Nernstian calibration characteristics of the electrode; hence, signals obtained at low $[Cl^-]_e$ yield greater signal differentials than those at high $[Cl^-]_e$. The flux values obtained from this data set, shown in Fig. 3B, reflect the biological signal *per se*. A net Cl^- influx was observed; it was maximal at 400 pmol cm^{-2} s^{-1} at $[Cl^-]_e$ values of 50 mmol l^{-1} or below. As

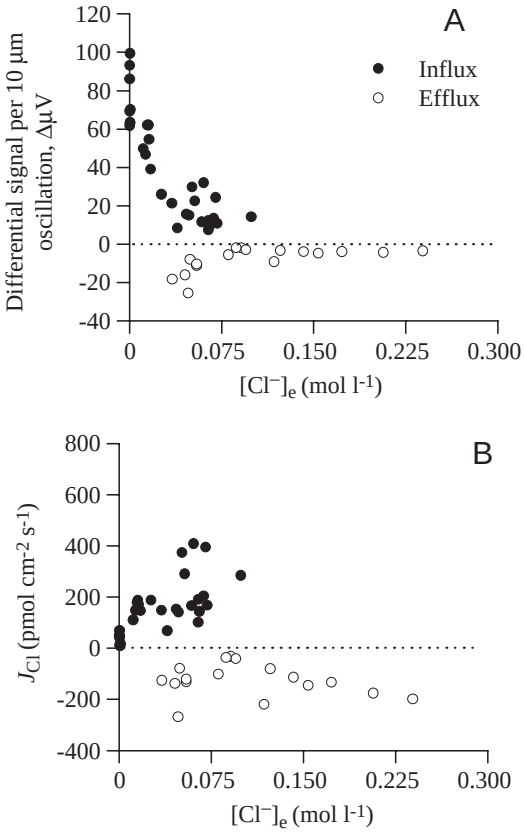

Fig. 3. Effects of $[Cl^-]_e$ on the differential signal (ΔμV) (A) and Cl^- flux (J_{Cl}) (B) from day 20 foetal distal lung epithelial cells (FDLEs). Cl^--selective microelectrode operating conditions are as given in Fig. 2. Each symbol represents the mean of at least 100 data points collected from FDLE cultures in steady state over a range of $[Cl^-]_e$. Filled symbols, cultures demonstrating a net Cl^- influx; open circles, cultures demonstrating a net Cl^- efflux.

$[Cl^-]_e$ was raised beyond this range, so J_{Cl} converted to a continuous efflux, becoming maximal at 203 pmol cm^{-2} s^{-1} at $[Cl]_e$ values greater than 100 mmol l^{-1}. Interestingly, between 50 and 100 mmol l^{-1} $[Cl^-]_e$, the direction of flux did not appear to vary predictably with $[Cl^-]_e$, with monolayers demonstrating Cl^- transport in either direction. Further investigation of this phenomenon revealed that the direction of spontaneously generated J_{Cl} was uniform from region to region within each monolayer, but that variance existed between separate monolayers even when the cells had originally been derived from the same preparation and the culture conditions remained identical. The lack of evidence for variation in this variable within each monolayer attests to the capacity for cells in this preparation to form a functionally coordinated transporting epithelium. A similar culture-to-culture variation in spontaneous fluid transport has previously been noted in wild-type (non-cystic-fibrosis) cultures of human tracheal epithelial cells (Jiang et al., 1997) and, together with our observations, this raises the intriguing possibility that J_{Cl} and, by extension, fluid transport may vary quite substantially in direction and magnitude from one region of the lung to another over permissive ranges of $[Cl^-]$ in airway liquid. The mechanism behind this requires further investigation. The observation that Cl^- is transported in an apical-to-basolateral direction at $[Cl^-]_e$<50 mmol l^{-1} may be explained by the apparent K_m of the basolateral $Na^+/K^+/2Cl^-$ cotransporter for Cl^-, which is 67 mmol l^{-1} in kidney epithelia (c.f. 1.3 mmol l^{-1} for K^+ and 7 mmol l^{-1} for Na^+) (Kaji, 1993). Assuming a similar kinetic profile for the basolateral cotransporter in lung epithelia, this would suggest that values of $[Cl^-]_e$ lower than 67 mmol l^{-1} would become rate-limiting for basolateral K^+ and Na^+ entry, thereby increasing the driving force for cation influx (Whisenant et al., 1993) and passive movement of Cl^- through the tight junctions. Notably, in a separate series of experiments, we have found that inhibition of the cotransporter with 25 μmol l^{-1} bumetanide invariably resulted in a large Cl^- influx irrespective of prevailing $[Cl^-]_e$ (the difference between bumetamide-inhibited and control J_{Cl} was +13.2±9.5 nmol cm^{-2} s^{-1}, mean ± S.E.M., N=3).

The dose- and $[Cl^-]_e$-dependent effects of Cl^- channel blockers (DPC and NPPB) on J_{Cl} are shown multi-dimensionally in Fig. 4A–C. As shown in Fig. 3, an increase in $[Cl^-]_e$ resulted in a stimulation of Cl^- efflux, which became increasingly responsive to inhibition by DPC at high $[Cl^-]_e$ (Fig. 4A). At any given $[Cl^-]_e$, Cl^- flux was inhibited maximally by up to 60 % at DPC concentrations equal to or greater than 10 μmol l^{-1} (Fig. 4B). Cl^- channel blockade by 10 μmol l^{-1} NPPB produced a suppression similar to that of J_{Cl} by DPC of up to 10 μmol l^{-1} for $[Cl^-]_e \geqslant 50$ mmol l^{-1} (Fig. 4C). Because the calibration properties of the electrodes were maintained over $[DPC] \leqslant 100$ μmol l^{-1} and $[NPPB] \leqslant 10$ μmol l^{-1}, measurements obtained outside these concentration ranges were discarded as unreliable.

Stimulation of Cl^- transport by β_2-adrenergic activation

Activation of β_2-adrenergic receptors in the pre-term foetal lung stimulates active Na^+ absorption, which provides the driving force for fluid clearance from the lung at birth (for a review, see Kemp and Olver, 1996). It has also been widely reported that this function is preserved in preparations of foetal distal lung epithelia (e.g. Ramminger et al., 1999), so we sought to determine the effect of β_2-adrenergic activation on the magnitude and direction of J_{Cl} that accompanies this Na^+ influx. Fig. 5 shows two non-identical representative experiments that detail the response of J_{Cl} to the β_2-adrenergic agonist isoproterenol. Whereas apical administration of 100 μmol l^{-1} isoproterenol had no effect, basolateral administration of 1–100 μmol l^{-1} isoproterenol activated a net Cl^- influx of 561 pmol cm^{-2} s^{-1}; this was inhibited by 50 % on addition of DPC. In cultures maintained at $[Cl^-]_e$>55 mmol l^{-1}, where a spontaneous Cl^- efflux was detected, the effect of isoproterenol was to stimulate a switch-over towards an obligatory, sustained Cl^- influx (Fig. 5, lower panel) that was maximal at 10 μmol l^{-1} isoproterenol.

The Cl^- SrE can resolve both passive and active ionic movements, so the isoproterenol-stimulated Cl^- absorption noted here presumably results from the movement of Cl^- consequent to the stimulation of Na^+ absorption. It is normally assumed that this passive movement of Cl^- occurs *via*

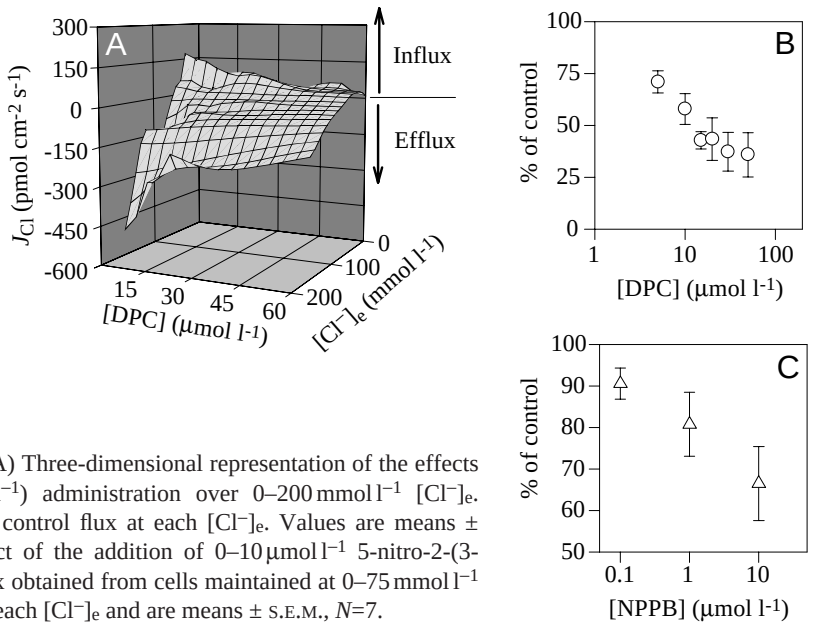

Fig. 4. Effects of Cl^- channel blockade on Cl^- flux (J_{Cl}). (A) Three-dimensional representation of the effects of diphenylamine-2-carboxylic acid (DPC) (0–60 μmol l^{-1}) administration over 0–200 mmol l^{-1} $[Cl^-]_e$. (B) Compiled data showing blockade as a percentage of control flux at each $[Cl^-]_e$. Values are means ± S.E.M., N=15. (C) Compiled data demonstrating the effect of the addition of 0–10 μmol l^{-1} 5-nitro-2-(3-phenylpropylamino)benzoic acid (NPPB) on apical Cl^- flux obtained from cells maintained at 0–75 mmol l^{-1} $[Cl^-]_e$. Results are expressed as a percentage of controls at each $[Cl^-]_e$ and are means ± S.E.M., N=7.

epithelial tight junctions and, as such, would not be responsive to Cl^- channel blockade. However, both the isoproterenol-stimulated Cl^- influx and its abrogation by DPC were conserved over a range of external Cl^- concentrations and were repeatable between individual FDLE preparations (Fig. 6A,B). Moreover, NPPB administered at 10 μmol l^{-1} tended to suppress isoproterenol-stimulated J_{Cl}, albeit without attaining statistical significance.

The action of DPC in reducing the isoproterenol-stimulated Cl^- absorption reported here is intriguing and could be explained in a variety of ways. (i) DPC may act on apical cation channels (Ruckes et al., 1997). We have recently noted, however, that isoproterenol-stimulated Na^+ absorption in monolayers maintained under short-circuit conditions is not affected by subsequent addition of DPC (A. Collett and S .M. Wilson, unpublished observations). (ii) DPC may decrease the anionic

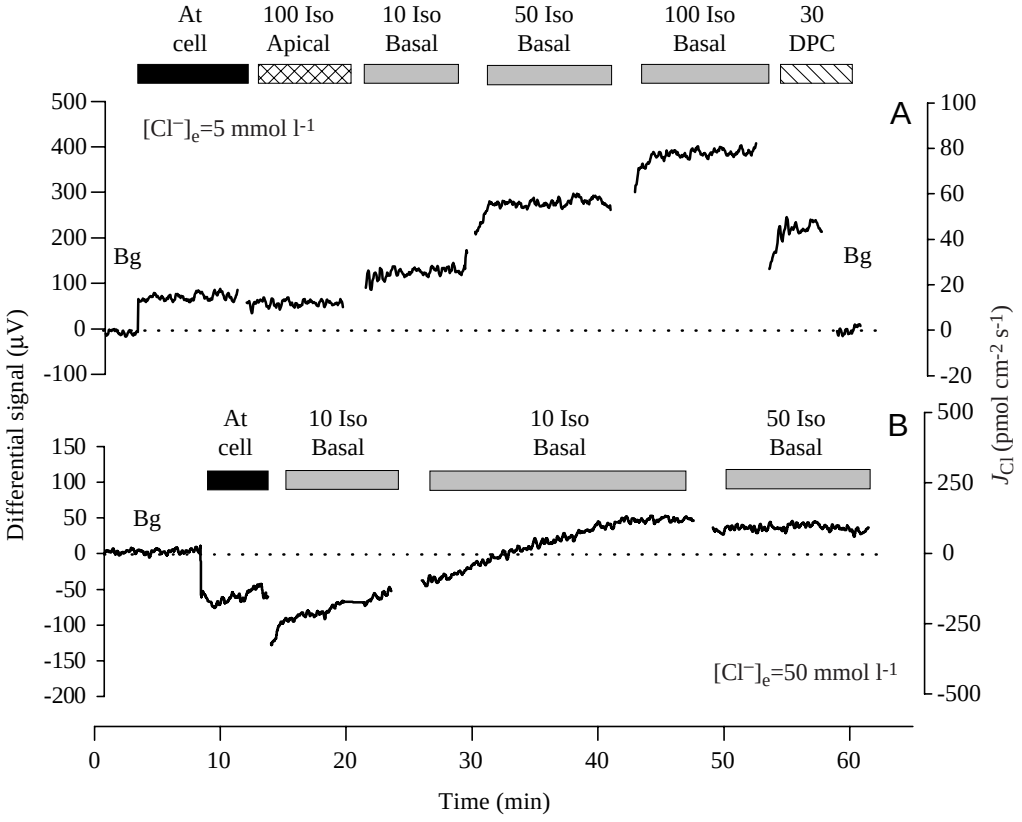

Fig. 5. Non-identical representative experiments demonstrating the effects of basolateral β_2-adrenergic blockade on signal differential and calculated Cl^- flux (J_{Cl}) at 5 mmol l^{-1} (A) and 50 mmol l^{-1} (B) $[Cl^-]_e$. At cell, point of closest approach to the apical aspect of a single cell within the monolayer; Bg, background measurement obtained 200 μm away from point of closest approach to the monolayer; Iso, isoproterenol. All concentrations of isoproterenol (Iso) and diphenylamine-2-carboxylic acid (DPC) are given in μmol l^{-1}.

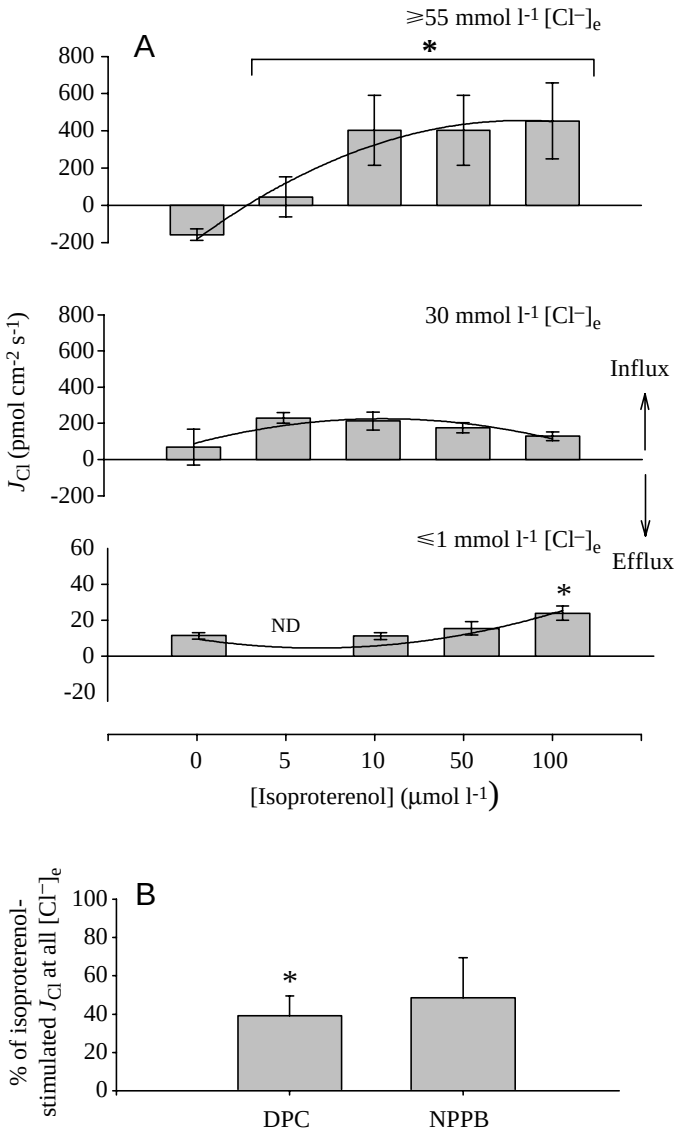

Fig. 6. (A) Compiled data demonstrating the effects of basolateral β_2-adrenergic activation by the addition of isoproterenol at concentrations increasing from 0 to 100 μmol l^{-1}on J_{Cl} at ≤1 (lower), 30 (middle) and ≥55 mmol l^{-1} (upper) $[Cl^-]_e$. Values are means ± S.E.M., N=4. Statistical significance (*P<0.05) was assessed relative to the control (0 μmol l^{-1} isoproterenol) group at each $[Cl^-]_e$ by one-way ANOVA with *post-hoc* significance assessed using Dunnett's test. (B) Compiled data from all external Cl^- concentrations demonstrating the effects of diphenylamine-2-carboxylic acid (DPC) (30 μmol l^{-1}) and 5-nitro-2-(3-phenylpropylamino)benzoic acid (NPPB) (10 μmol l^{-1}) on isoproterenol-stimulated Cl^- flux. Values are means ± S.E.M. (N=7 for DPC; N=3 for NPPB). Significance (denoted by an asterisk) was assessed at 95 % relative to 100 μmol l^{-1} isoproterenol treatment using a paired Student's t-test.

permeability of the tight junctions, but this explanation is inconsistent with observations that DPC has little effect on the basal transepithelial resistance (R_t) in monolayers of these cells (Ramminger et al., 1999). (iii) DPC has been reported to have inhibitory effects on the basolateral K^+ conductance required to maintain a potential difference favouring Na^+ absorption (Richards and Dawson, 1993). It is conceivable, therefore, that the inhibition of isoproterenol-stimulated Cl^- transport by DPC may result from a slowing of the passive movement of Cl^- along a diminished Na^+ gradient. (iv) The passive movement of anions occurs *via* a transcellular route through apical anion channels. This would require a basolateral Cl^- conductance coupled with tight junctions, which are relatively impermeable to Cl^- (Uyekubo et al., 1998). The range of R_t we report (approximately 300 Ω cm^2), however, suggests that the monolayers we used were relatively freely permeable. It is interesting to note that Jiang et al. (Jiang et al., 1998) have reported that β_2-adrenergic activation with terbutaline results in an increase in apical Cl^- permeability as a precursor to the activation of a Na^+ conductance. Furthermore, Uyekubo et al. (Uyekubo et al., 1998) have noted that forskolin treatment of high-resistance monolayers of tracheal epithelial cells induces fluid absorption that is abrogated by 100 μmol l^{-1} NPPB. These studies support a transcellular model for Cl^- transport favouring either a basolateral KCl cotransporter (Jiang et al., 1998) or basolateral Cl^- channels (Uyekubo et al., 1998) as the means for Cl^- exit from the cell. Although this fits with our observations, further experiments are required to elucidate this effect with the Cl^- SrE.

Stimulation of Cl^- flux by $P2Y_2$ receptor activation

P2 purinoceptors are ubiquitously distributed in epithelia and characteristically evoke the release of Ca^{2+} from intracellular stores *via* phospholipase C (PLC) when activated by ATP or UTP. Although the physiological role of P2 receptors in secretory epithelia remains a subject of debate, a clear consequence of ATP administration to the apical membranes of normal and cystic fibrosis transmembrane conductance regulator (CFTR)-deficient epithelia is to stimulate Cl^- efflux and fluid secretion (Mason et al., 1991). Consequently, P2Y receptors constitute part of an autocrine signalling mechanism that is an attractive target for the manipulation of fluid secretion in diseases associated with defective Cl^- transport.

Previous work has demonstrated that rat FDLEs express $P2Y_2$ receptors in the apical membrane when cultured on permeable supports under the conditions used in this study (Clunes et al., 1998). In view of the capacity of ATP and UTP to activate Cl^- secretion, we undertook to characterise the Cl^--dependency of UTP-evoked Cl^- flux in isolated FDLEs. Fig. 7A demonstrates the effect of UTP administration (10–500 μmol l^{-1}) upon the steady-state direction and magnitude of Cl^- flux in FDLE monolayers. In keeping with the basal unstimulated data in Figs 2 and 3, low external concentrations of Cl^- resulted in a net Cl^- absorption, which switched towards a net Cl^- secretion upon addition of UTP, yielding a maximal flux of 300 pmol cm^{-2} s^{-1} at 100 μmol l^{-1} (UTP) and 150 mmol l^{-1} $[Cl^-]_e$. However, this response was diminished when UTP concentrations were increased to 500 μmol l^{-1}, with J_{Cl} not significantly different from baseline conditions. Administration of DPC tended to suppress UTP-stimulated J_{Cl}. However, the results we obtained did not achieve statistical significance (Fig. 7B). Recent studies

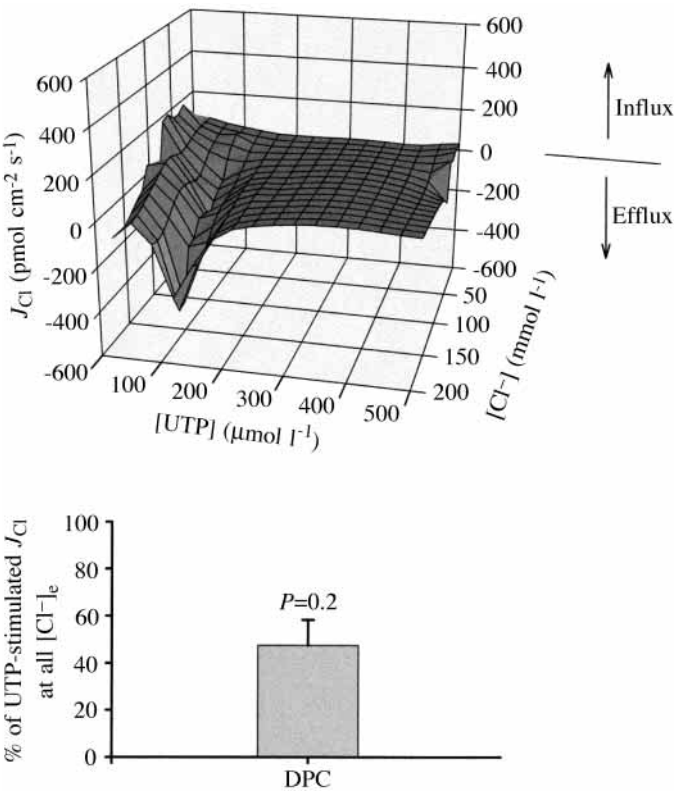

Fig. 7. (A) Three-dimensional representation of the $[Cl^-]_e$-dependence of UTP-stimulated Cl^- secretion. Data obtained from cells treated with 0, 10, 50, 100, 200 and 500 μmol l^{-1} UTP over the course of 23 separate experiments were used to create a mathematically interpolated three-dimensional mesh. (B) Compiled data from all external Cl^- concentrations demonstrating the effects of diphenylamine-2-carboxylic acid (DPC) (30 μmol l^{-1}) on UTP-stimulated Cl^- flux (J_{Cl}). Values are means + S.E.M. (N=9, DPC). Significance was assessed at 95 % relative to 100 μmol l^{-1} UTP treatment using paired Student's t-test.

based in bronchial epithelia have demonstrated that a cessation of Na^+ absorption accompanies UTP-evoked Cl^- secretion (Inglis et al., 1999). We found that Na^+ channel blockade with 10 μmol l^{-1} amiloride substantially increased the maximal stimulation of Cl^- efflux observed with 100 μmol l^{-1} UTP at high $[Cl^-]_e$ (Table 2). This observation is in broad agreement with work on upper airway epithelia suggesting that Na^+ channel blockade results in a hyperpolarisation of the apical membrane, thus increasing the driving force for Cl^- out of the cell (Clarke and Boucher, 1992; Inglis et al., 1999). Together with the Cl^- influx observed in the isoproterenol experiments, these results demonstrate the utility of Cl^--selective SrEs in assessing the directional regulation of Cl^- transport as a function of $[Cl^-]_e$ and, by extension, the physiology of fluid transport.

Concluding remarks

A Cl^--selective self-referencing microelectrode has been developed that can be used to determine the directional flux of Cl^- from individual epithelial cells maintained in monolayer culture. Spontaneous Cl^- transport was detected as a function of the Nernstian characteristics of the electrode over values of $[Cl^-]_e$ between 0.5 and 210 mmol l^{-1}. Although the physiological concentration of Cl^- in the alveolus is a matter of debate, we have used this approach to demonstrate that the pharmacological responsiveness of apical J_{Cl} to adrenergic and purinergic receptor agonists varies in both magnitude and direction according to $[Cl^-]_e$ at the external surface of the plasma membrane. The fact that we can detect a dynamic gradient of Cl^- attests to the inadequacy of bulk $[Cl^-]$ as a predictor of actual $[Cl^-]$ within the microenvironment of the plasma membrane. This is important for the understanding of the cellular and molecular processes associated with epithelial fluid transport that are ostensibly regulated according to the concentration of salts in the airway surface liquid.

This work was conducted during a research visit to the BioCurrents Research Center, Marine Biological Laboratory, Woods Hole, MA 02543, USA (Director Dr P. J. S. Smith, supported by NIH-NCRR). Our thanks to their staff for providing expert technical assistance and an efficient, friendly working environment. We also thank Drs Sarah Inglis, Sophia Jovanovic and Stuart Wilson for their helpful comments on the manuscript. Supported by grants from the Royal Society and the Medical Research Council (S.C.L.).

Table 2. *Effect of UTP and amiloride on the relationship between J_{Cl} and $[Cl^-]_e$*

Condition	a (pmol cm^{-2} s^{-1})	b	r^2	P for F, regression	P for convariance *versus* control
Control	202.6±25.4	−2.3±0.3	0.61	<0.001	–
Amiloride (10 μmol l^{-1})	90.6±24.3	−1.50±0.4	0.81	0.014	NS
UTP (100 μmol l^{-1})	103.5±28.3	−3.05±0.4	0.74	<0.001	<0.05
UTP+amiloride	256.2±114.5	−5.06±1.6	0.72	0.031	<0.05

The relationship between J_{Cl} and $[Cl^-]_e$ is expressed as $J_{Cl}=a–b[Cl^-]_e$.

Values represent respective line coefficients ± S.E.M.; N=41 (controls), N=6 (amiloride), N=22 (UTP) and N=6 (UTP+amiloride).

Analysis of covariance ($F_{3,69}$=8.17, H_o: $\beta_{Control}=\beta_{Amiloride}=\beta_{UTP}=\beta_{UTP+Amiloride}$ rejected) followed by Dunn's test was used to assess differences among treatments relative to the control group with confidence limits set to 95 %.

NS, not significantly different.

References

Baconnais, S., Tirouvanziam, R., Zahm, J. M., de Bentzmann, S., Peault, B., Balossier, G. and Puchelle, E. (1999). Ion composition and rheology of airway liquid from cystic fibrosis fetal tracheal xenografts. *Am. J. Respir. Cell Mol. Biol*. **20**, 605–611.

Boucher, R. C. (1994). Human airway ion transport. I. *Am. J. Respir. Crit. Care Med*. **150**, 271–281.

Boucher, R. C. (1999). Molecular insights into the physiology of the 'thin film' of airway surface liquid. *J. Physiol., Lond.* **516**, 631–638.

Breton, S., Smith, P. J. S., Lui, B. and Brown, D. (1996). Acidification of the male reproductive tract by a proton-pumping ATPase. *Nature Medicine* **2**, 470–472.

Clarke, L. L. and Boucher, R. C. (1992). Chloride secretory response to extracellular ATP in human normal and cystic fibrosis nasal epithelia. *Am. J. Physiol*. **265**, C348–C356.

Clunes, M. T., Collett, A., Baines, D. L., Bovell, D. L., Murphie, H., Inglis, S. K., McAlroy, H. L., Olver, R. E. and Wilson, S. M. (1998). Culture substrate-specific expression of P2Y(2) receptors in distal lung epithelial cells isolated from foetal rats. *Br. J. Pharmac.* **124**, 845–847.

Hull, J., Skinner, W., Robertson, C. and Phelan, P. (1998). Elemental content of airway surface liquid from infants with cystic fibrosis. *Am. J. Respir. Crit. Care Med.* **157**, 10–14.

Illek, B., Tam, A.W., Fischer, H. and Machen, T. E. (1999). Anion selectivity of apical membrane conductance of Calu 3 human airway epithelium. *Pflügers Arch.* **437**, 812–822.

Illek, B., Yankaskas, J. R. and Machen, T. E. (1997). cAMP and genistein stimulate HCO_3^- conductance through CFTR in human airway epithelia. *Am. J. Physiol*. **272**, L752–L761.

Inglis, S. K., Collett, A., McAlroy, H. L., Wilson, S. M. and Olver, R. E. (1999). Effect of luminal nucleotides on Cl^- secretion and Na^+ absorption in distal bronchi. *Pflügers Arch.* **438**, 621–627.

Jaffe, L. F. and Nuccitelli, R. (1974). An ultrasensitive vibrating probe for measuring steady extracellular currents. *J. Cell Biol*. **63**, 614–628.

Jiang, C., Finkbeiner, W. E., Widdicombe, J. H. and Miller, S. S. (1997). Fluid transport across cultures of human tracheal glands is altered in cystic fibrosis. *J. Physiol., Lond.* **501**, 637–647.

Jiang, X., Ingbar, D.H. and O'Grady, S M.. (1998). Adrenergic stimulation of Na^+ transport across alveolar epithelial cells involves actibation of apical Cl^- channels. *Am. J. Physiol*. **275**, C1610–C1620.

Kaji, D. M. (1993). $Na^+/K^+/2Cl^-$ cotransport in medullary thick ascending limb cells: Kinetics and bumetanide binding. *Biochim. Biophys. Acta* **1152**, 289–299.

Kemp, P. J. and Olver, R. E. (1996). The cellular basis of G protein regulation of alveolar ion channels. *Exp. Physiol*. **81**, 493–593.

Knowles, M. R., Robinson, J. M., Wood, R. E., Pue, C. A., Mentz, W. M., Wager, G. C., Gatzy, J. T. and Boucher, R. C. (1997). Ion composition of airway surface liquid of patients with cystic fibrosis as compared with normal and disease-control subjects. *J. Clin. Invest.* **100**, 2588–2595.

Kondo, Y., Buhrer, T., Seiler, K., Fromter, E. and Simon, W. (1989). A new double-barrelled, ionophore-based microelectrode for chloride ions. *Pflügers Arch.* **414**, 663–668.

Kuhtreiber, W. M. and Jaffe, L. F. (1990). Detection of extracellular calcium gradients with a calcium-specific vibrating electrode. *J. Cell Biol.* **110**, 1565–1573.

Land, S. C., Porterfield, D. M., Sanger, R. H. and Smith, P. J. S. (1999). The self-referencing oxygen-selective microelectrode: detection of transmembrane O_2 flux from single cells. *J. Exp. Biol.* **202**, 211–218.

Land, S. C., Sanger, R. H. and Smith, P. J. S. (1997). O_2-availability modulates transmembrane Ca^{2+}-flux *via* second-messenger pathways in anoxia-tolerant hepatocytes. *J. Appl. Physiol.* **82**, 776–783.

Mason, S. J., Paradiso, A. M. and Boucher, R. C. (1991). Regulation of transepithelial ion transport and intracellular calcium by extracellular ATP in human and cystic fibrosis airway epithelium. *Br. J. Pharmac.* **103**, 1649–1656.

Matsui, H., Grubb, B. R., Tarran, R., Randell, S. H., Gatzy, J. T., Davis, C. W. and Boucher, R. C. (1998). Evidence for periciliary liquid layer depletion, not abnormal ion composition, in the pathogenesis of cystic fibrosis airways disease. *Cell* **95**, 1005–1015.

Muller-Berger, S., Samarzija, I., Kunimi, M., Yamada, H., Fromter, E. and Seki. G. (1999). A stop-flow microperfusion technique for rapid determination of HCO_3^- absorption/H^+-secretion by isolated renal tubules. *Pflügers Arch.* **439**, 208–215.

Ramminger, S., Collett, A., Baines, D. L., Murphie, H., McAlroy, H. L., Olver, R. E., Inglis, S. K. and Wilson, S. M. (1999). $P2Y_2$ receptor-mediated inhibition of ion transport in distal lung epithelial cells. *Br. J. Pharmac.* **128**, 293–300.

Richards, N. W. and Dawson, D. C. (1993). Selective block of specific K^+-conducting channels by diphenylamine-2-carboxylate in turtle colon epithelial cells. *J. Physiol., Lond.* **462**, 715–734.

Ruckes, C., Blank, U., Moller, K., Rieboldt, J., Lindemann, H., Munker, G., Clauss, W. and Weber, W.-M. (1997). Amiloride-sensitive Na^+ channels in human nasal epithelium are different from classical epithelial Na^+ channels. *Biochem. Biophys. Res. Commun.* **237**, 488–491.

Schellhase, D. E., Emrie, P. A., Fisher, J. H. and Shannon, J. M. (1989). Ontogeny of surfactant apoproteins in the rat. *Ped. Res.* **26**, 167–174.

Shirihai, O., Smith, P. J. S., Hammar, K. and Dagan, D. (1998). H^+ and K^+ gradient generated by microglia H/K ATPase. *Glia* **23**, 339–348.

Smith, P. J. S., Sanger, R. H. and Jaffe, L. F. (1994). The vibrating Ca^{2+} electrode: A new technique for detecting plasma membrane regions of Ca^{2+} influx and efflux. In *Methods in Cell Biology. A Practical Guide to the Study of Ca^{2+} in Living Cells* (series ed. L. Wilson and P. Matsudaira; volume ed. R. Nuccitelli), **40**, 115–134. San Diego: Academic Press.

Smith, P. J. S. and Trimarchi, J. R. (2000). Non-invasive measurement of hydrogen and potassium ion flux from single cells and epithelial structures. *Am. J. Physiol.* (in press).

Trimarchi, J. R., Liu, L., Porterfield, D. M., Smith, P. J. S. and Keefe, D. L. (2000). Oxidative phosphorylation-dependent and -independent oxygen consumption by individual preimplantation mouse embryos. *Biol. Reprod.* **62**, 1866–1874.

Tsuruoka, S. and Schwartz, G. J. (1999). Mechanisms of HCO_3^- secretion in the rabbit connecting segment. *Am. J. Physiol*. **277**, F567–F574.

Uyekubo, S. N, Fischer, H., Maminishkis, A., Illek, B., Miller, S. S. and Widdicombe, J. H. (1998). cAMP-dependent absorption of chloride across airway epithelium. *Am. J. Physiol.* **275**, L1219–L1227.

Whisenant, N., Khademazad, M. and Muallem, S. (1993). Regulatory interaction of ATP, Na^+ and Cl^- in the turnover cycle of the $Na^+/K^+/2Cl^-$ cotransporter. *J. Gen. Physiol*. **101**, 889–908.